

## Two-quasiproton states in $^{190}\text{Os}$ and $^{192}\text{Os}$ studied with the $(t, \alpha)$ reaction

R. D. Bagnell, Y. Tanaka,\* and R. K. Sheline  
Florida State University, Tallahassee, Florida 32306

D. G. Burke  
McMaster University, Hamilton, Ontario, Canada

J. D. Sherman†  
Los Alamos Scientific Laboratory, Los Alamos, New Mexico 87545  
(Received 8 May 1978; revised manuscript received 4 December 1978)

Level structures up to 3000 keV in  $^{190}\text{Os}$  and  $^{192}\text{Os}$  have been studied using the  $^{191}\text{Ir}$  and  $^{193}\text{Ir}$   $(t, \alpha)$  proton pickup reactions with 15 MeV tritons. The  $\alpha$ -particle spectra were obtained with the quadrupole-dipole-dipole-dipole magnetic spectrometer with peak widths of  $\sim 11$  keV (full width half maximum). This reaction strongly excites the  $I, K^\pi = 4, 4^+$  levels at 1162 keV in  $^{190}\text{Os}$  and at 1070 keV in  $^{192}\text{Os}$ , which were previously interpreted as two-phonon  $\gamma$ -vibrational states. The large two-quasiproton amplitude is reasonably explained by assuming single-phonon hexadecapole vibrations which involve the  $\{5/2 [402], 3/2 [402]\}$  configuration. Many two-quasiproton states are observed in the energy region 2000–3000 keV. The strongest peaks found at an excitation energy of  $\sim 2600$  keV in both  $^{190}\text{Os}$  and  $^{192}\text{Os}$  may be the remaining portions of the two-quasiproton  $\{5/2 [402], 3/2 [402]\}_{I, K^\pi = 4, 4^+}$  states.

NUCLEAR REACTIONS  $^{191, 193}\text{Ir}(t, \alpha)^{190, 192}\text{Os}$ ,  $E_t = 15$  MeV; measured  $\sigma(E_\alpha)$ ; enriched targets; analyses, DWBA including the  $(t - \alpha - \alpha')$  channel, the strong coupling model, RPA.

### I. INTRODUCTION

The even osmium nuclei lie in the transition region between nuclei with permanent deformation and those with spherical equilibrium shape. The presence of very low lying  $K^\pi = 2^+$  vibrational bands implies that the  $\gamma$  degree of freedom is quite important in these nuclei. The hexadecapole degree of freedom may also be important as pointed out in Refs. 1 and 2. Owing to these properties, the osmium nuclei have been the subject of a wide variety of experimental and theoretical studies. Experimentally,  $^{190}\text{Os}$  has been studied through Coulomb excitation,<sup>3,4</sup> radioactive decay,<sup>5,6</sup> neutron capture  $\gamma$  ray,<sup>7,8</sup> inelastic  $\alpha$ -particle scattering,<sup>2,9</sup> and single neutron<sup>10</sup> and two neutron transfer reactions.<sup>11–13</sup>  $^{192}\text{Os}$  has been studied using Coulomb excitation,<sup>3,4</sup> radioactive decay,<sup>14</sup> inelastic  $\alpha$ -particle scattering,<sup>2</sup> and  $(t, p)$  experiments.<sup>13</sup> The  $(t, \alpha)$  proton pickup reaction employed in the present studies has the potential to study two-quasiproton states of  $^{190, 192}\text{Os}$  from the microscopic point of view.

Bands with  $K^\pi = 2^+$ , explained as single-phonon  $\gamma$  vibrations, are observed at excitation energies of  $\sim 500$  keV in both nuclei. At approximately twice the single-phonon energy there is a set of states which has been described as the  $0^+$  and  $4^+$  two-phonon doublets.<sup>11</sup> The  $I, K^\pi = 4, 4^+$  states given

this designation occur at 1162 keV in  $^{190}\text{Os}$  and 1070 keV in  $^{192}\text{Os}$ . In addition to the good energy agreement with harmonic vibrator predictions for two-phonon states and the correct value for the  $K$  projection quantum number, these states were populated, at most, very weakly in neutron transfer reactions. The 1162 keV state in  $^{190}\text{Os}$  was not observed in the  $^{189}\text{Os}(d, p)$  reaction<sup>10</sup> and was only weakly populated in the  $^{192}\text{Os}(p, t)$  and  $^{188}\text{Os}(t, p)$  spectra.<sup>11–13</sup> The 1070 keV level in  $^{192}\text{Os}$  was excited, at most, very weakly in the  $^{190}\text{Os}(t, p)$  reaction.<sup>13</sup> In view of the two-phonon interpretation, it is therefore surprising that these states are strongly populated in the present experiments. In each spectrum there are also many strongly populated levels observed in the energy region 2000–3000 keV. The most reasonable interpretation of these states is that they come from two-quasiproton configurations since they lie above the pairing gap  $2\Delta \sim 1600$  keV determined from the mass tables.<sup>15</sup> Although none of these higher lying levels has known spin and parity, possible Nilsson configurations are discussed for some of them based on their  $(t, \alpha)$  cross sections.

### II. EXPERIMENTAL PROCEDURES AND RESULTS

The experiments were performed using 15 MeV tritons from the Fn tandem Van de Graaff accelera-

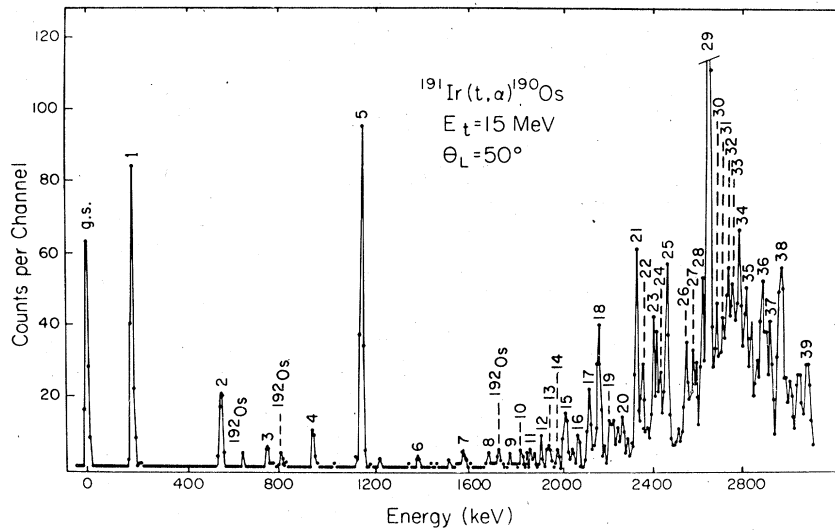


FIG. 1. The  $\alpha$ -particle spectrum for the  $^{191}\text{Ir}(t, \alpha)^{190}\text{Os}$  reaction at  $50^\circ$ .

tor at the Los Alamos Scientific Laboratory. The targets were made at Florida State University by evaporating iridium metal samples, isotopically enriched to 94.6% for  $^{191}\text{Ir}$  and to 98.7% for  $^{193}\text{Ir}$ , onto carbon foils. The target thicknesses were  $43 \mu\text{g}/\text{cm}^2$  for  $^{191}\text{Ir}$  and  $37 \mu\text{g}/\text{cm}^2$  for  $^{193}\text{Ir}$ . Charged particles produced in the reactions were analyzed using the quadrupole-dipole-dipole-dipole (Q3D) magnetic spectrometer and detected with a 50 cm helical-cathode position-sensitive counter on the focal plane.<sup>16</sup> Particle identification was achieved by measuring  $\Delta E/\Delta X$  in the counter gas and the total energy in a plastic scin-

tillator in which the particles were stopped. The range of excitation energies which could be measured at one time with the 50 cm detector was  $\sim 1.7$  MeV. In order to obtain spectra up to  $\sim 4$  MeV excitation, three overlapping segments were recorded with the detector moved to different positions along the focal plane. Measurements were made at angles of  $\theta = 40^\circ$  and  $\theta = 50^\circ$  for each target and the peak widths were  $\sim 11$  keV full width at half maximum (FWHM) for all runs. Figures 1 and 2 show the alpha-particle spectra at  $50^\circ$  for  $^{190}\text{Os}$  and  $^{192}\text{Os}$ , respectively. The intensities of peaks in these spectra were converted to cross

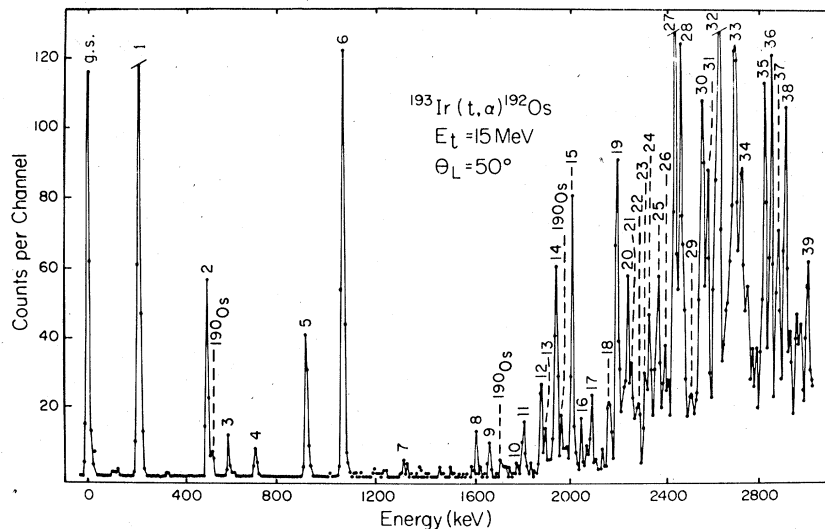


FIG. 2. The  $\alpha$ -particle spectrum for the  $^{193}\text{Ir}(t, \alpha)^{192}\text{Os}$  reaction at  $50^\circ$ .

TABLE I. Levels populated in  $^{190}\text{Os}$ .

Level number	Level energy (keV)	Cross sections ( $\mu\text{b}/\text{sr}$ )		Level number	Level energy (keV)	Cross sections ( $\mu\text{b}/\text{sr}$ )	
		$\theta = 40^\circ$	$\theta = 50^\circ$			$\theta = 40^\circ$	$\theta = 50^\circ$
g. s.	0	23.2	22.1	21	2327	18.5	19.0
1	185	26.8	28.7	22	2354	9.1	10.6
2	556	8.7	9.2	23	2409	16.6	24.2
3	755	1.7	2.4	24	2437	13.9	13.1
4	955	4.7	4.4	25	2463	29.3	27.4
5	1162	31.7	27.8	26	2535	10.4	10.5
6	1388	1.0	0.9	27	2568	11.5	10.3
7	1573	1.6	1.8	28	2629	21.1	21.4
8	1684	1.3	1.1	29	2655	69.2	75.5
9	1778	3.4	2.4	30	2690	29.6	31.2
10	1825	1.3	2.1	31	2719	24.3	22.2
11	~1870	2.3	1.8	32	2741	25.0	28.6
multiplet							
12	1910	3.1	2.5	33	2773	21.0	25.6
13	1939	2.5	3.4	34	2791	27.8	25.4
14	1980	2.4	1.5	35	2815	24.1	24.7
15	2015	5.2	6.4	36	2885	23.2	27.8
16	2071	4.1	3.5	37	2914	14.4	12.8
17	2120	8.1	8.0	38	2963	29.9	39.9
18	2163	17.1	18.3	39	3076	10.9	19.3
19	2219	10.4	10.9	40	3455	13.3	26.8
20	2267	5.5	6.0				

sections by using a silicon monitor counter of known solid angle in the target chamber to record elastically scattered tritons at  $30^\circ$ . The elastic scattering cross section at  $30^\circ$  was obtained from

an optical model calculation using parameters reported by Flynn et al.<sup>17</sup> for elastic scattering of tritons from  $^{182}\text{W}$ . It was found that the use of other triton parameter sets, which had been obtained

TABLE II. Levels populated in  $^{192}\text{Os}$ .

Level number	Level energy (keV)	Cross sections ( $\mu\text{b}/\text{sr}$ )		Level number	Level energy (keV)	Cross sections ( $\mu\text{b}/\text{sr}$ )	
		$\theta = 40^\circ$	$\theta = 50^\circ$			$\theta = 40^\circ$	$\theta = 50^\circ$
g. s.	0	31.3	31.3	20	2258	11.8	14.2
1	208	35.3	37.9	21	2276	4.2	9.8
2	490	11.0	12.1	22	2304	4.9	4.3
3	580	1.6	1.8	23	2337	6.7	5.0
4	691	2.5	2.5	24	2352	12.7	13.5
5	911	8.8	9.7	25	2392	8.3	13.1
6	1070	28.8	29.3	26	2423	8.6	14.0
7	1348	2.7	1.5	27	2466	36.4	35.5
8	1613	2.1	2.4	28	2489	22.7	26.4
9	1667	1.7	2.0	29	2508	14.6	15.2
10	1780	1.3	1.5	30	2619	25.3	30.2
11	1809	3.0	3.1	31	2643	21.2	22.5
12	1883	4.3	5.1	32	2686	54.5	59.9
13	1903	3.2	3.4	33	2756	45.6	45.6
14	1945	16.7	18.5	34	2788	22.7	28.4
15	2016	16.7	17.9	35	2887	29.6	36.7
16	2058	2.9	3.2	36	2916	31.1	34.4
17	2096	3.3	4.5	37	2947	21.4	18.1
18	2176	6.2	7.3	38	2978	25.7	25.0
19	2210	21.2	24.2	39	3088	10.3	9.4

from fits to triton scattering data, resulted in negligible changes ( $\approx 2\%$ ) in the calculated elastic scattering cross section at  $\theta = 30^\circ$  for the present study. The relative intensities measured in this way are reliable to within  $\pm 10\%$  but the absolute cross sections have larger uncertainties of the order of  $\pm 20\%$ . Excitation energies were determined using a quadratic calibration polynomial obtained by recording spectra from the  $^{153}\text{Eu}(t, \alpha)^{152}\text{Sm}$ ,  $^{166}\text{Er}(t, \alpha)^{165}\text{Ho}$ , and  $^{190}\text{Os}(t, \alpha)^{189}\text{Re}$  reactions immediately before the present exposures. The excitation energies and cross sections for levels in  $^{190}\text{Os}$  and  $^{192}\text{Os}$  are presented in Tables I and II. The experimental uncertainties on the excitation energies for strong transitions are  $\pm 4$  keV for levels below 1 MeV in excitation,  $\pm 6$  keV for levels between 1 and 2 MeV, and  $\pm 8$  keV for higher levels.

### III. INTERPRETATION AND DISCUSSION

Figures 1 and 2 and Tables I and II indicate that the intensities of the  $I, K^\pi = 4, 4^+$  levels<sup>14,18</sup> (the no. 5 level at 1162 keV in  $^{190}\text{Os}$  and the no. 6 level at 1070 keV in  $^{192}\text{Os}$ ) are comparable to those of the ground states. As these are among the largest peaks in the spectra, the  $I, K^\pi = 4, 4^+$  levels must contain fairly large two-quasiproton amplitudes. The most likely two-quasiproton configuration involves the coupling of the  $\frac{3}{2}[402]$  target proton with the  $\frac{5}{2}[402]$  excited proton orbital. The latter should be a low lying proton hole state in this region of nuclei since it is the ground state configuration for most of the odd- $A$  rhenium ( $Z = 75$ ) isotopes. There are no other Nilsson states expected to yield such large cross sections to  $I, K^\pi = 4, 4^+$  states in the  $(t, \alpha)$  reaction.

There has been some difference of opinion<sup>14,19</sup> on the possible existence of a state in  $^{190}\text{Os}$  at 1782 keV with tentative spin and parity of  $4^-$ . The  $(t, \alpha)$  reaction weakly populates a level at 1778 keV which may correspond to the 1782 keV level. Although this is not a strong argument in itself, four previously unassigned  $\gamma$  transitions<sup>14</sup> populate and depopulate a level at  $1780.2 \pm 0.2$  keV. Spin  $3^\pm$  is implied by the pattern of population and de-

population if dipole radiation is assumed.

Distorted-wave Born-approximation (DWBA) cross sections for the present study were computed with the Program DWUCK.<sup>20</sup> The optical potential parameters from the  $(\alpha, t)$  studies of Lu and Alford<sup>21</sup> were used. Although these parameters, shown in Table III, were not obtained from fits to elastic scattering data, they have been found<sup>22</sup> to give better fits to  $(t, \alpha)$  angular distributions than other optical parameters which were based on scattering data. The relative spectroscopic strengths obtained using these parameters with  $(\alpha, t)$  data from tungsten<sup>21</sup> and osmium<sup>23</sup> targets were also in good agreement with those from  $(^3\text{He}, d)$  results. There are fairly large uncertainties in the absolute normalization factor,  $N$ , which is used in  $(t, \alpha)$  analyses, due mainly to ambiguities in the  $\alpha$  parameters. In several recent  $(t, \alpha)$  studies involving targets of erbium, osmium, and platinum, it was found<sup>24,25</sup> that values of  $N = 32$  to 35 were required with these optical parameters, in order that reasonable spectroscopic strengths be obtained for some known states. In the present study a value of  $N = 40$  has been used so that the strengths of the ground state transitions are consistent with those obtained from the inverse  $(^3\text{He}, d)$  reactions.<sup>23</sup> In view of the rather large uncertainties ( $\sim 30$  to  $50\%$ ) involved in extracting spectroscopic strengths from  $(t, \alpha)$  data<sup>22</sup> at the present time, the value of 40 is considered to be consistent with the values of 32–35 mentioned above.

For the DWBA calculations no lower cutoff was applied in the radial integration, no nonlocal parameters were used, and the form factor for a Woods-Saxon potential with uniform charge distribution was assumed. Typical angular distributions are shown in Fig. 3 for each transfer angular momentum. Beyond  $\sim 20^\circ$  there is little shape difference between these curves. These structureless angular distributions are typical for reactions involving large momentum mismatches. The only difference in the distributions is in the relative magnitude of their cross sections.

The strong coupling model<sup>26,27</sup> was used to obtain the spectroscopic amplitudes. For odd- $A$  iri-

TABLE III. Optical potential parameters used in the DWBA calculations.

	$V_0$	$r_0$	$a$	$W_0$	$W_D$	$r'_0$	$a'$	$V_{so}$	$r_c$
$t$	200.0	1.40	0.60	50.0	0	1.40	0.60	0	1.30
$\alpha$	200.0	1.40	0.60	20.0	0	1.40	0.60	0	1.30
bound state	a	1.25	0.65	0	0	0	0	3.0	1.25

<sup>a</sup> Adjusted to reproduce the separation energy.

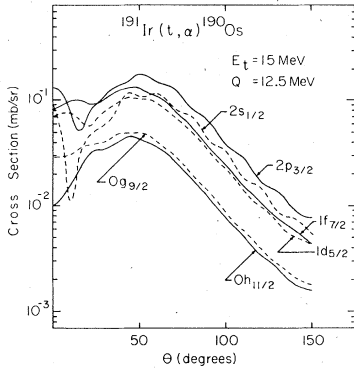


FIG. 3. Calculated angular distributions for the  $^{191}\text{Ir}(t, \alpha)^{190}\text{Os}$  reaction. Optical potential parameters are given in Table III.  $N=40$  is assumed for the normalization factor for the  $(t, \alpha)$  reaction.

dium nuclei, the Hamiltonian includes rotation-particle and particle- $\gamma$  vibration coupling effects. The strength of the latter coupling is determined from the observed  $B(E2)$  value<sup>4</sup> between the  $\gamma$  vibration and the ground state in the respective osmium nucleus. A single-particle wave function is constructed from the Nilsson potential with axial symmetry<sup>28,29</sup> and is written in terms of the spherical shell model basis as

$$|\Omega\rangle = \sum_j C_{j\Omega} |j\Omega\rangle. \quad (1)$$

The ground state wave function of the target nucleus is then given as

$$|I'M'\rangle = \sum_{K'\Omega n'_2} C_{K'\Omega n'_2} |I'M'K'\Omega n'_2\rangle \quad (2)$$

and

$$|I'M'K'\Omega n'_2\rangle = \left(\frac{2I'+1}{16\pi^2}\right)^{1/2} \times [D_{M'K'}^{I'+K'} a_{\Omega}^{\dagger} + (-1)^{I'+K'} D_{M'-K'}^{I'+K'} a_{\Omega}^{\dagger}] |n'_2\rangle. \quad (3)$$

Here  $n'_2 (\leq 1)$  is the number of  $\gamma$  phonons,  $a^{\dagger}$  is the creation operator of a quasiparticle, and  $|\bar{\Omega}\rangle$  is the time reversal state with respect to the state  $|\Omega\rangle$ .

On the other hand, the  $\gamma$  vibration in the even osmium nuclei is constructed by using the random-phase approximation (RPA) formalism with the quadrupole interaction between quasiparticles. The  $\gamma$  phonon  $A_{\gamma}^{\dagger}$  is thus given by

$$A_{\gamma}^{\dagger} = \sum_{p,q} X_{pq} A_{p,q}^{\dagger} + \sum_{p,q} Y_{pq} A_{p,q} \quad (4)$$

and

$$A_{p,q}^{\dagger} = a_p^{\dagger} a_q^{\dagger}. \quad (5)$$

In Eq. (4),  $X_{pq}$  ( $Y_{pq}$ ) is the forward (backward) amplitude for the two-quasiparticle states  $p$  and  $q$ . The wave function for the ground and  $K^{\pi} = 2^+$  band members is written as

$$|IMKn_2\rangle = \left[\frac{2I+1}{16\pi^2(1+\delta_{K0})}\right]^{1/2} \{D_{MK}^{I+K} + (-1)^{I+K} D_{M-K}^{I+K}\} |n_2\rangle \quad (6)$$

and  $n_2 (\leq 1)$  is the number of  $\gamma$  phonons.

The  $K^{\pi} = 4^+$  bands lie considerably below the energy gap, the observed  $(t, \alpha)$  strengths populating them are significantly less than expected in the DWBA calculation assuming the pure  $\left\{\frac{3}{2}[402], \frac{5}{2}[402]\right\}$  configuration, and the levels are populated weakly but significantly in inelastic  $\alpha$ -particle scattering experiments.<sup>2,9</sup> All of these facts suggest a considerable degree of collectivity in the  $K^{\pi} = 4^+$  bands. Since the two-phonon states are composed in general of four-quasiparticle configurations, such levels should not be populated strongly in single nucleon transfer reactions on targets in which the odd nucleons are in pure single-particle states. In order to explain the present  $(t, \alpha)$  cross sections for these states in terms of the two-phonon  $\gamma$  vibrations, the target ground states would have to consist of particles coupled to single-phonon  $\gamma$  vibrations. This situation is highly unlikely, since the  $^{190,192}\text{Os}(\alpha, t)^{191,193}\text{Ir}$  reactions<sup>23</sup> show that the ground states of the Ir nuclei are predominantly single-quasiparticle states. One would also imagine that the  $(t - \alpha - \alpha')$  two-step process via the  $I, K^{\pi} = 2, 2^+$  state might explain the  $I, K^{\pi} = 4, 4^+$  cross section. However, it is also quite unlikely, since the two-step cross section would only be  $\sim 0.1 \mu\text{b}$  using the experimental  $B(E2)$  values<sup>4</sup> and the calculated two-step cross section for the  $I, K^{\pi} = 2, 0^+$  state discussed later. In addition, the  $K^{\pi} = 4^+$  two-phonon state would be shifted above twice the single-phonon energy, owing to the fact that a fair portion of the  $K^{\pi} = 4^+$  wave function may violate the Pauli exclusion principle<sup>30</sup> because of the aligned  $K$  quantum number of two  $\gamma$  phonons. Thus it is quite probable that the  $K^{\pi} = 4^+$  band is a two-quasiparticle collective mode, i.e., a single-phonon hexadecapole vibration.<sup>31,32</sup> In view of the above arguments, four-quasiparticle amplitudes would at most be a minor portion of the  $K^{\pi} = 4^+$  wave function. The hexadecapole vibration is constructed in a similar fashion to the  $\gamma$  vibration, using the hexadecapole interaction between quasiparticles. Finally, noncollective two-quasiproton states observed in the high energy portion of the spectra are assumed to have a pure two-quasiproton configuration, i.e.,

$$|IMK\Omega_p\Omega_q\rangle = \left(\frac{2I+1}{16\pi^2}\right)^{1/2} \{D_{MK}^{I*} a_p^\dagger a_q^\dagger - (-1)^{I+K} D_{M-K}^{I*} a_p^\dagger a_q^\dagger\} |0\rangle. \quad (7)$$

The state with  $K = \Omega_p + \Omega_q$  may be written in a similar way.

Using the above wave functions, the spectroscopic amplitudes for the  $K^\pi = 0^+$  and  $K^\pi = 2^+$  band mem-

bers are written as

$$\beta_{nIj} = \left[\frac{2I+1}{(2I'+1)(1+\delta_{K0})}\right]^{1/2} \sum_{K'\Omega_n} \delta_{n_2 n_2'} C_{K'\Omega_n} U_{\Omega} C_{j\Omega} \{(IKj\Omega|I'K') + (-1)^{I+K} (I-Kj\Omega|I'K')\}, \quad (8)$$

while for the  $K^\pi = 2^+$  and  $K^\pi = 4^+$  band members,

$$\beta_{nIj} = -\left(\frac{2I+1}{2I'+1}\right)^{1/2} \sum_{K'\Omega_n} \delta_{n_2' 0} C_{K'\Omega_n} \sum_{pq} X_{pq} \{\delta_{p\Omega} V_q C_{jq} (IKjq|I'K') + (-1)^{I+K} \delta_{q\Omega} V_p C_{jp} (I-Kjp|I'K')\}. \quad (9)$$

The spectroscopic amplitude for the  $K^\pi = 2^+$  band members should be calculated using the sum of Eqs. (8) and (9) due to the presence of the single-phonon  $\gamma$ -vibrational amplitude in the ground state wave function of the target nucleus. Equation (9) may also be used for transitions to noncollective two-quasiproton states, provided that the summation with respect to  $p$  and  $q$  is omitted and  $X_{pq}$  is set equal to unity.

In the above calculation, the harmonic oscillator potential is determined by the usual constants<sup>29</sup>  $\kappa^p = \kappa^n = 0.0637$ ,  $\mu^p = 0.60$ ,  $\mu^n = 0.42$ , and  $\hbar\omega = 41.2 A^{-1/3}$  MeV. The strengths of the quadrupole interaction and the hexadecapole interaction, used to construct the  $\gamma$  vibration and the hexadecapole vibration, are determined in such a way as to give the experimental band head energies. Wave functions are solved in the harmonic oscillator space of  $N=4, 5$  for protons and  $N=5, 6$  for neutrons. The deformation parameter  $\beta_2$  is fixed as 0.165 for  $^{191}\text{Ir}$  and  $^{190}\text{Os}$  and 0.145 for  $^{193}\text{Ir}$  and  $^{192}\text{Os}$ . Positive deformation is implied from the observed quadrupole moments for the  $I, K^\pi = 2, 0^+$  states in  $^{190,192}\text{Os}$ .<sup>33</sup> Positive deformation is also assumed for  $^{191,193}\text{Ir}$ , since

this assumption gave successful results in the analysis of  $^{190,192}\text{Os}(\alpha, t)^{191,193}\text{Ir}$  reactions.<sup>23</sup> The pairing interactions  $G_p$  and  $G_n$  are adjusted to give the empirical gap energies from the mass tables.<sup>15</sup> The Coriolis force and the particle- $\gamma$  vibration coupling need to be reduced by 50% in order to give cross sections consistent with experiments. Coriolis attenuation factors of this magnitude are common in this region. Furthermore, the makeup of the two-quasiparticle components of the  $\gamma$ -vibration limits the availability for occupation by the odd- $A$  particles, leading to the needed reduction of the particle- $\gamma$  vibration coupling. The particle can be thought of as being blocked by the  $\gamma$  phonon. Some of the calculated wave functions are shown in Table IV.

In Tables V and VI, calculated cross sections are compared with experimental values for low lying rotational band members in  $^{190}\text{Os}$  and  $^{192}\text{Os}$ , respectively. As mentioned above, the normalization factor of  $N \sim 40$  was chosen in order to explain the ground state transition strength. It is perhaps rather fortuitous that the calculated cross sections shown in Tables V and VI for the  $I, K^\pi = 4,$

TABLE IV. Calculated wave functions for the ground state of  $^{191}\text{Ir}$ , the  $\gamma$  vibration of  $^{190}\text{Os}$ , and the hexadecapole vibration of  $^{190}\text{Os}$ . Forward amplitudes are given for these vibrations.

$$\begin{aligned} |^{191}\text{Ir: g. s.}\rangle &= 0.96\{-\frac{3}{2}[402]\}_r - 0.11\{\frac{1}{2}[400]\}_r \\ &\quad + 0.23\{\frac{1}{2}[400]\}_r \otimes (\gamma \text{ vib.}) \\ |^{190}\text{Os: } K^\pi = 2^+\rangle &= 0.47\{\frac{5}{2}[402], \frac{1}{2}[400]\}_r + 0.44\{\frac{1}{2}[400], -\frac{3}{2}[402]\}_r \\ &\quad + 0.70\{\frac{1}{2}[510], -\frac{3}{2}[512]\}_r + 0.43\{-\frac{3}{2}[501], -\frac{7}{2}[503]\}_r \\ &\quad + (3 \text{ terms around } 0.3) \\ |^{190}\text{Os: } K^\pi = 4^+\rangle &= 0.61\{\frac{5}{2}[402], -\frac{3}{2}[402]\}_r + 0.41\{\frac{1}{2}[501], -\frac{7}{2}[503]\}_r \\ &\quad + (4 \text{ terms between } 0.3 \text{ and } 0.4) \end{aligned}$$

TABLE V. Comparison of experimental and calculated cross sections for low lying rotational band members of  $^{190}\text{Os}$ .

$I, K^\pi$	Level no.	Excitation energy (keV)	Reaction cross sections ( $\mu\text{b}/\text{sr}$ )			
			40° Exp.	Cal. <sup>a</sup>	50° Exp.	Cal. <sup>a</sup>
0, 0 <sup>+</sup>	g. s.	0	23.2	26.6	22.1	26.6
2, 0 <sup>+</sup>	1	185	26.8	23.0	28.7	23.0
				[37.6] <sup>b</sup>		[34.4] <sup>b</sup>
4, 0 <sup>+</sup>	2	556	1.1 <sup>c</sup>	1.0	1.2 <sup>c</sup>	1.0
2, 2 <sup>+</sup>	2	556	7.6 <sup>c</sup>	10.6	8.0 <sup>c</sup>	10.7
3, 2 <sup>+</sup>	3	755	1.7	1.5	2.4	1.5
4, 2 <sup>+</sup>	4	955	4.7	1.2	4.4	1.1
4, 4 <sup>+</sup>	5	1162	31.7	27.9	27.8	27.6

<sup>a</sup> $N=40$  is assumed for the normalization factor of the  $(t, \alpha)$  reaction.

<sup>b</sup>Cross sections in brackets include the two-step contribution.

<sup>c</sup>Cross sections determined by using the same ratio as that in  $^{192}\text{Os}$ .

4<sup>+</sup> states agree so well with the experimental values, especially as the uncertainties involved in the  $(t, \alpha)$  reaction mechanism can affect the calculated intensities significantly. However, these effects, which may be of the order of 30% to 50%, can in no way obscure the main feature of this discussion—namely that the cross sections for the  $I, K^\pi = 4, 4^+$  states are consistent with the presence of a large  $\{\frac{5}{2} + [402] + \frac{3}{2} + [402]\}_{K=4}$  two-quasiproton admixture (as predicted for a hexadecapole interpretation) but are orders of magnitude larger than expected for the two-phonon configuration.

In addition, using the hexadecapole interaction,

$$H_{\text{int}} = \frac{1}{2}K_4(Y_4Y_4), \quad (10)$$

the Hartree-Fock potential is calculated as

$$V_4^{\text{HF}} = K_4 \sum_i \langle i | r^4 Y_{40} | i \rangle. \quad (11)$$

On the other hand, the nuclear shape is given by

$$R = R_0(1 + \beta_2 Y_{20} + \beta_4 Y_{40}) \quad (12)$$

and the corresponding hexadecapole potential is

$$V = -m\omega^2 \beta_4 \frac{r^4}{R_0^2} Y_{40}. \quad (13)$$

By comparing Eq. (12) and Eq. (13), the deformation  $\beta_4$  may be connected with the strength  $K_4$  as<sup>34</sup>

$$\beta_4 = -\frac{2mR_0^2}{\hbar^2} K_4 \sum_{i>0} V_i^2 \langle i | r^4 Y_{40} | i \rangle. \quad (14)$$

Here  $K_4 \approx -5200 A^{-3} \text{ MeV}$  and  $R_0 = 1.2 A^{1/3} \text{ fm}$ .

The value of  $\beta_4 = -0.025$  obtained by this procedure is consistent with the prediction of negative  $\beta_4$  values in nuclei around  $A = 190$ , and is consistent with the values of  $|\beta_4| \sim 0.02$  obtained for these states in recent  $(\alpha, \alpha')$  experiments.<sup>9</sup> The small  $|\beta_4|$  value implies that the strength  $K_4$  is reasonable and the hexadecapole vibration may well appear in the energy region around 1100 keV.

TABLE VI. Comparison of experimental and calculated cross sections for low lying rotational band members of  $^{192}\text{Os}$ .

$I, K^\pi$	Level no.	Excitation energy (keV)	Reaction cross sections ( $\mu\text{b}/\text{sr}$ )			
			40° Exp.	Cal. <sup>a</sup>	50° Exp.	Cal. <sup>a</sup>
0, 0 <sup>+</sup>	g. s.	0	31.3	30.7	31.3	30.8
2, 0 <sup>+</sup>	1	208	35.3	24.6	37.9	24.5
				[37.9] <sup>b</sup>		[34.9] <sup>b</sup>
4, 0 <sup>+</sup>	3	580	1.6	0.9	1.8	0.9
2, 2 <sup>+</sup>	2	490	11.0	12.7	12.1	12.5
3, 2 <sup>+</sup>	4	691	2.5	1.4	2.5	1.4
4, 2 <sup>+</sup>	5	911	8.8	1.1	9.7	1.1
4, 4 <sup>+</sup>	6	1070	28.8	27.9	29.3	27.7

<sup>a</sup> $N=40$  is assumed for the normalization factor of the  $(t, \alpha)$  reaction.

<sup>b</sup>Cross sections in brackets include the two-step contribution.

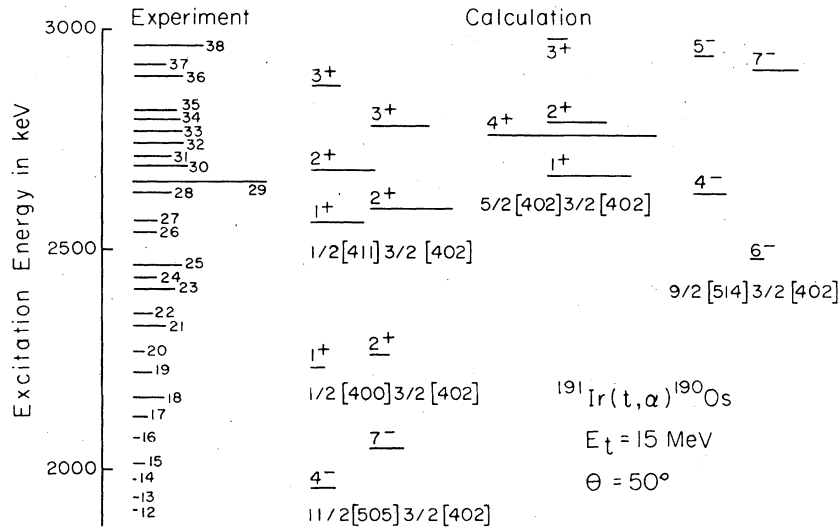


FIG. 4. Calculated and experimental cross sections at  $50^\circ$  for states within the energy region of 2000–3000 keV in  $^{190}\text{Os}$ .

Two-step processes involving inelastic excitation via the ground states of  $^{190,192}\text{Os}$  are important in explaining the cross sections for the  $I, K^\pi = 2, 0^+$  states. In both nuclei, the second member of the ground state rotational band was populated to a greater extent than the ground state, although the single-step calculation predicts a smaller strength for the  $I, K^\pi = 2, 0^+$  state. The direct plus two-step contributions were calculated by the program TWOSTEP,<sup>35</sup> using first and second order distorted-wave Born approximations. Cross sections including this process are given in brackets

in Tables V and VI and are seen to be 50% larger than those for the single-step process.

In the high energy portion of each spectrum, many levels are strongly populated. Although none of these levels has known spin and parity, it might be possible to guess possible two-quasiproton configurations for some of the levels by comparing their cross sections with calculations. Figures 4 and 5 show these comparisons for  $^{190}\text{Os}$  and  $^{192}\text{Os}$ , respectively. Predicted excitation energies are calculated as the sum of two-quasiparticle energies and rotational kinetic energies. No configura-

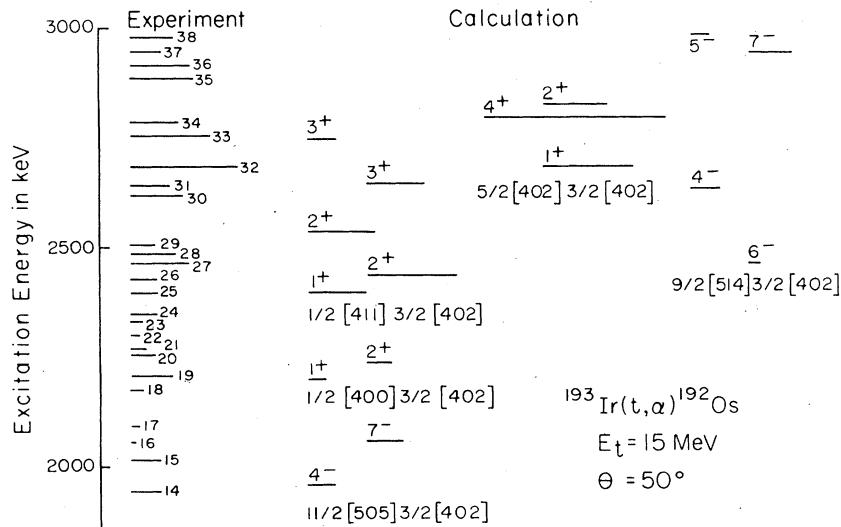


FIG. 5. Calculated and experimental cross sections at  $50^\circ$  for states within the energy region of 2000–3000 keV in  $^{192}\text{Os}$ .



tion mixing is assumed and the interaction between the two quasiparticles is also omitted.

Figures 4 and 5 imply that the two-quasiproton configurations populated in the  $(t, \alpha)$  reaction in this energy region are expected to involve the coupling of the  $\frac{3}{2}[402]$  orbital with the five Nilsson orbitals,  $\frac{11}{2}[505]$ ,  $\frac{9}{2}[514]$ ,  $\frac{1}{2}[400]$ ,  $\frac{1}{2}[411]$ , and  $\frac{5}{2}[402]$ . Levels above 2500 keV might be expected to be rotational members of the  $\{\frac{1}{2}[411], \frac{3}{2}[402]\}$ ,  $\{\frac{5}{2}[402], \frac{3}{2}[402]\}$ , and  $\{\frac{9}{2}[514], \frac{3}{2}[402]\}$  configurations, while levels below 2500 keV would reasonably be rotational band members of the  $\{\frac{11}{2}[505], \frac{3}{2}[402]\}$  and  $\{\frac{1}{2}[400], \frac{3}{2}[402]\}$  configurations. The most strongly populated levels, no. 29 in  $^{190}\text{Os}$  and no. 32 in  $^{192}\text{Os}$ , would be interpreted as the  $\{\frac{5}{2}[402], \frac{3}{2}[402]\}_{I, K^\pi=4, 4^+}$  states. Although  $\sim 35\%$  of this strength as seen from Table IV is shifted to the low lying  $I, K^\pi = 4, 4^+$  hexadecapole vibrational state, the remaining strength would explain the observed cross sections.

The antiparallel coupling of the  $\{\frac{5}{2}[402], \frac{3}{2}[402]\}$  configuration gives rise to a rotational band with  $K^\pi = 1^+$ . This band can be fairly easily confused both in energy and cross sections with the  $K^\pi = 1^+$  band arising from the  $\{\frac{1}{2}[411], \frac{3}{2}[402]\}$  configuration. Recognizing these difficulties, we find that it is not possible to make reliable assignments for any other two-quasiproton states on the basis of the present data only. However, it is clear that in both  $^{190}\text{Os}$  and  $^{192}\text{Os}$  there are several combinations of levels between  $\sim 2400$  keV and  $\sim 3000$  keV which have populations similar to those predicted for the  $\{\frac{5}{2}[402], \frac{3}{2}[402]\}_{K=1}$ ,  $\{\frac{1}{2}[411], \frac{3}{2}[402]\}_{K=1}$ , and  $\{\frac{1}{2}[411], \frac{3}{2}[402]\}_{K=2}$  configurations. To identify some of these levels it would be useful to perform the  $(t, \alpha)$  reaction with polarized tritons as the transfer of the  $\frac{5}{2}[402]$  proton is predominantly  $j^\pi = \frac{5}{2}^+$  whereas most of the strength in the  $\frac{1}{2}[411]$  transfer is  $j^\pi = \frac{3}{2}^+$ . Recent  $(\bar{t}, \alpha)$  studies<sup>36</sup> on osmium targets have shown that these cases can be readily distinguished from the signs of the analyzing powers.

#### IV. SUMMARY

The present results have shown that the low lying rotational band members in  $^{190}\text{Os}$  and  $^{192}\text{Os}$  are satisfactorily explained in the present model. The

unusually good agreement with the experimental cross sections for the  $I, K^\pi = 4, 4^+$  states at 1162 keV in  $^{190}\text{Os}$  and at 1070 keV in  $^{192}\text{Os}$  implies that these states can be explained as single-phonon hexadecapole vibrations. Recent results from  $(\alpha, \alpha')$  experiments<sup>9</sup> support the interpretation given in the present work. Although these two experiments imply that the  $K = 4^+$  bands in  $^{192, 190}\text{Os}$  have a large amplitude of hexadecapole vibration, they do not exclude the possibility of a significant additional amplitude of two-phonon  $\gamma$  vibration in these same bands. The experimental method of this paper is a probe for two-quasiproton configurations which are interpreted in terms of the hexadecapole vibration. They say nothing about the amplitude of the two-phonon vibration. However, the systematic evidence<sup>10, 37, 38</sup> for the preferential  $\gamma$  decay of the  $K = 4^+$  bands to the  $K = 2^+$  one-phonon  $\gamma$ -vibrational bands implies that these are not pure hexadecapole vibrations. The decay of a hexadecapole vibration to the one-phonon  $\gamma$  vibration should be forbidden since it requires the destruction of one phonon and the creation of a radically different one.

The evidence for a two-phonon  $\gamma$ -vibration amplitude in the  $K = 4^+$  bands presented in the Introduction is heightened by recent work<sup>37, 38</sup> that includes new data in  $^{192, 190}\text{Os}$  and an alternate theoretical interpretation in terms of the new interacting boson model of Arima and Iachello. The success of this model in predicting the experimentally observed changing depopulation of the  $K = 4^+$  bands to band members of the  $K = 2^+$  one-phonon bands argues strongly for its essential correctness. However, the  $K = 4^+$  bands in the interacting boson model are the geometrical analogs of the two-phonon  $\gamma$  vibrations. Thus it seems probable that the  $K = 4^+$  bands in  $^{192, 190}\text{Os}$  are quite complex and contain large amplitudes of both the two-phonon  $\gamma$  vibrations and the one-phonon hexadecapole vibration.

The authors are grateful for the opportunity to use the facilities at the Los Alamos Van de Graaff Laboratory. The cooperation of O. Hansen, E. Flynn, J. Sunier, S. Orbesen, and R. Woods was particularly helpful for the success of these experiments and is appreciated very much. This work was supported by ERDA and the NSF.

\*Present address: Department of Physics, Tokyo Institute of Technology, Meguro, Tokyo, Japan.

†Present address: Accelerator Technology Division, Los Alamos Scientific Laboratory, Los Alamos, New Mexico 87545.

<sup>1</sup>D. L. Hendrie, N. K. Glendenning, B. G. Harvey, O. N.

Jarvis, H. H. Duhm, J. Mahoney, and J. Saudinos, in *Proceedings of the International Conference on Nuclear Structure, Tokyo, 1967*, edited by J. Sawada (Univ. of Tokyo Press, Tokyo, Japan, 1967), p. 306.

<sup>2</sup>F. T. Baker, T. H. Kruse, W. Hartwig, I. Y. Lee, and J. X. Saladin, *Nucl. Phys. A258*, 43 (1976).

- <sup>3</sup>W. T. Milner, F. K. McGowan, R. L. Robinson, P. H. Stelson, and R. O. Sayer, Nucl. Phys. A177, 1 (1971).
- <sup>4</sup>R. F. Casten, J. S. Greenberg, S. H. Sie, G. A. Burginon, and D. A. Bromley, Phys. Rev. 187, 1532 (1969).
- <sup>5</sup>P. E. Haustein and A. F. Voigt, Nucl. Phys. A136, 414 (1969).
- <sup>6</sup>T. Yamazaki, H. Ikegami, and M. Sakai, Nucl. Phys. A131, 169 (1969).
- <sup>7</sup>M. A. Mariscotti, W. R. Kane, and G. T. Emery, Report No. BNL-11426, 1967 (unpublished).
- <sup>8</sup>E. Bohm and K. Stelzer, in *Proceedings of the International Symposium on Neutron Capture Gamma-Ray Spectroscopy, Studsvik, 1969* (International Atomic Energy Agency, Vienna, 1969), p. 403.
- <sup>9</sup>D. G. Burke, M. A. M. Shahabuddin, and R. N. Boyd, Phys. Lett. 78B, 48 (1978).
- <sup>10</sup>S. W. Yates, J. C. Cunnane, P. J. Daly, R. Thompson, and R. K. Sheline, Nucl. Phys. A222, 276 (1974).
- <sup>11</sup>H. L. Sharma and N. M. Hintz, Phys. Rev. C 13, 2288 (1976); Phys. Rev. Lett. 31, 1517 (1973).
- <sup>12</sup>R. C. Thompson, J. S. Boyno, J. R. Huizenga, D. G. Burke, and Th. W. Elze, Nucl. Phys. A242, 1 (1975).
- <sup>13</sup>E. R. Flynn and D. G. Burke, Phys. Rev. C 17, 501 (1978).
- <sup>14</sup>M. R. Schmorak, Nucl. Data Sheets 9, 195 (1973).
- <sup>15</sup>A. H. Wapstra and N. G. Gove, Nucl. Data Tables 9, 267 (1971).
- <sup>16</sup>E. R. Flynn, S. Orbesen, J. D. Sherman, J. W. Sunier, and R. Woods, Nucl. Instrum. 128, 35 (1975).
- <sup>17</sup>E. R. Flynn, D. D. Armstrong, J. G. Beery, and A. G. Blair, Phys. Rev. 182, 1113 (1969).
- <sup>18</sup>M. R. Schmorak, Nucl. Data Sheets 9, 401 (1973).
- <sup>19</sup>L. Samuelsson, R. Vukanović, M. Migahed, M. Zupancic, L. O. Edvardson, and L. Westerberg, Nucl. Phys. A135, 657 (1969).
- <sup>20</sup>P. D. Kunz, University of Colorado (unpublished).
- <sup>21</sup>M. T. Lu and W. P. Alford, Phys. Rev. C 3, 1243 (1971).
- <sup>22</sup>D. G. Burke, G. Løvholden, E. R. Flynn, and J. W. Sunier, Phys. Rev. C 18, 693 (1978).
- <sup>23</sup>R. H. Price, D. G. Burke, and M. W. Johns, Nucl. Phys. A176, 338 (1971).
- <sup>24</sup>G. Løvholden, D. G. Burke, E. R. Flynn, and J. W. Sunier, Nucl. Phys. A303, 1 (1978).
- <sup>25</sup>Y. Yamazaki, R. K. Sheline, and D. G. Burke, Z. Phys. A285, 191 (1978).
- <sup>26</sup>A. Bohr, in K. Dan. Vidensk. Selsk., Mat.-Fys. Medd. 26, No. 14 (1952).
- <sup>27</sup>A. Bohr and B. R. Mottelson, in K. Dan. Vidensk. Selsk., Mat.-Fys. Medd. 27, No. 16 (1953).
- <sup>28</sup>S. G. Nilsson, in K. Dan. Vidensk. Selsk. Mat.-Fys. Medd. 29, No. 16 (1955).
- <sup>29</sup>W. Ogle, S. Wahlborn, R. Piepenbring, and S. Fredriksson, Rev. Mod. Phys. 43, 424 (1971).
- <sup>30</sup>J. D. Immele, Ph.D. thesis University of California, Berkeley, 1972 (unpublished).
- <sup>31</sup>R. D. Bagnell, Y. Tanaka, R. K. Sheline, D. G. Burke, and J. D. Sherman, Phys. Lett. 66B, 129 (1977).
- <sup>32</sup>R. H. Spear, J. P. Warner, A. M. Baxter, M. T. Esat, M. P. Fewell, S. Hinds, A. M. R. Joye, and D. C. Kean, Aust. J. Phys. 30, 133 (1977).
- <sup>33</sup>S. A. Lane and J. X. Saladin, Phys. Rev. C 6, 613 (1972).
- <sup>34</sup>K. Harada, Phys. Lett. 10, 80 (1964).
- <sup>35</sup>M. Igarashi and M. Toyama, Institute for Nuclear Study, University of Tokyo (unpublished).
- <sup>36</sup>C. R. Hirning, D. G. Burke, E. R. Flynn, J. W. Sunier, P. A. Schmelzbach, and R. F. Haglund, Jr., Nucl. Phys. A287, 24 (1977).
- <sup>37</sup>W. F. Davidson, Nucl. Phys. A309, 206 (1978).
- <sup>38</sup>R. F. Casten and J. A. Cizewski, Nucl. Phys. A309, 477 (1978).